

Local fluid dynamics in patients with bifurcated coronary lesions undergoing percutaneous coronary interventions

Lorenzo Genuardi^{1,2}, Yiannis S. Chatzizisis³, Claudio Chiastra⁴,
 Gregory Sgueglia⁵, Habib Samady⁶, Ghassan S. Kassab⁷,
 Francesco Migliavacca⁴, Carlo Trani^{1,2}, Francesco Burzotta^{1,2}

¹Fondazione Policlinico Universitario A. Gemelli IRCCS, Rome, Italy

²Institute of Cardiology, Università Cattolica del Sacro Cuore, Rome, Italy

³Cardiovascular Biology and Biomechanics Laboratory, Cardiovascular Division,
 University of Nebraska Medical Center, Omaha, NE, USA

⁴Laboratory of Biological Structure Mechanics (LaBS), Chemistry, Materials and Chemical
 Engineering “Giulio Natta” Department, Politecnico di Milano, Milan, Italy

⁵Division of Cardiology, Sant’Eugenio Hospital, Rome, Italy

⁶Andreas Gruentzig Cardiovascular Center, Division of Cardiology, Department of Medicine,
 Emory University School of Medicine, Atlanta, GA, USA

⁷California Medical Innovations Institute, San Diego, CA, USA

Abstract

Although the coronary arteries are uniformly exposed to systemic cardiovascular risk factors, atherosclerosis development has a non-random distribution, which follows the local mechanical stresses including flow-related hemodynamic forces. Among these, wall shear stress plays an essential role and it represents the major flow-related factor affecting the distribution of atherosclerosis in coronary bifurcations. Furthermore, an emerging body of evidence suggests that hemodynamic factors such as low and oscillating wall shear stress may facilitate the development of in-stent restenosis and stent thrombosis after successful drug-eluting stent implantation. Drug-eluting stent implantation represents the gold standard for bifurcation interventions. In this specific setting of interventions on bifurcated lesions, the impact of fluid dynamics is expected to play a major role and constitutes substantial opportunity for future technical improvement. In the present review, available data is summarized regarding the role of local fluid dynamics in the clinical outcome of patients with bifurcated lesions. (Cardiol J 2021; 28, 2: 321–329)

Key words: fluid dynamics, wall shear stress, coronary bifurcation lesions, percutaneous coronary intervention, bifurcation stenting, in-stent restenosis and thrombosis

Coronary bifurcation lesions: Complex structure

The epicardial coronary artery tree is an extremely complex vascular structure characterized by a high number of arterial branching points

where complex hemodynamic local conditions of blood flow facilitates atherogenesis. A bifurcation coronary lesion is a lesion occurring at, or adjacent to, a significant division of a major epicardial coronary artery [1]. Coronary bifurcation anatomy may basically be regarded as a complex vessel/function

Address for correspondence: Francesco Burzotta, MD, PhD, Institute of Cardiology, Fondazione Policlinico Universitario A. Gemelli IRCCS, Università Cattolica del Sacro Cuore. L.go Gemelli 8, 00168 Rome, Italy, tel: +393494295290, fax: +39063055535, e-mail: francescoburzotta@gmail.com

Received: 24.09.2019

Accepted: 25.01.2020

This article is available in open access under Creative Commons Attribution-Non-Commercial-No Derivatives 4.0 International (CC BY-NC-ND 4.0) license, allowing to download articles and share them with others as long as they credit the authors and the publisher, but without permission to change them in any way or use them commercially.

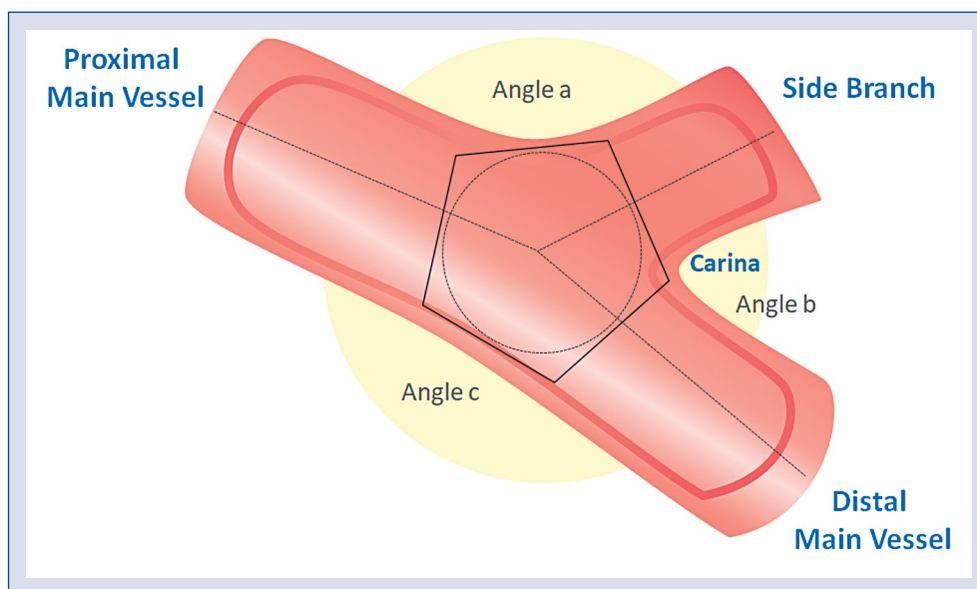


Figure 1. An idealized coronary artery bifurcation. The bifurcation anatomy is usually best described by the three segments model comprised of the proximal main vessel (MV), the distal MV and side branch (SB). The area comprised of the ideal interception between MV and SB is commonly identified as the polygon of confluence.

structure where three different vessel segments, namely proximal main vessel (MV), distal MV, and side branch (SB), are interpolated through the bifurcation core segment where the distinction between MV and SB is merely virtual (Fig. 1) [1]. The area comprised by the ideal interception between MV and SB is commonly identified as the polygon of confluence (Fig. 1). The carina represents the point at which the proximal MV divides into distal MV and SB, and has the critical functional role of splitting the antegrade flow (“flow divider”) (Fig. 1). Three angles (a, b, c) allows describing of the spatial orientation between the three bifurcation segments (Fig. 1).

Coronary bifurcations represent the target lesion in 15–20% of all percutaneous coronary interventions (PCI) and, due to their specific anatomic-functional features, remain a daily challenge in contemporary interventional cardiology practice [1]. Drug-eluting stent (DES) implantation early has become the gold standard for bifurcation PCI [2], but the search for the best implantation technique is an evolving field. Bifurcation PCI is associated with higher procedural complications and clinical adverse event risks [1, 3]. Local biomechanics, and fluid shear stresses in particular, appear to be implicated in the development of both in-stent restenosis (ISR) and stent thrombosis (ST) which usually explains the occurrence of adverse clinical events in PCI patients [4].

The purpose of this review is to summarize the available data regarding the role of local fluid dynamics in clinical outcomes of stented bifurcations.

Fluid dynamics at the level of coronary bifurcations

Atherosclerosis has a non-random distribution that reflects the local effect of flow-related biomechanical forces. In particular, atherosclerotic plaques usually develop in arterial segments where blood flow perturbations occur, including the ostia of branches, the inner side of curvatures and major bifurcations [5].

Among different coronary hemodynamic measures, shear stress (SS) is defined as the tangential stress derived from the friction of adjacent layers of blood flowing parallel to each other in the vessel path. The wall shear stress (WSS) is the shear stress acting on the luminal surface of the arterial wall and has a recognized impact on vessel wall biology [5]. Low WSS modulates endothelial gene expression through complex mechanoreception and mechanotransduction processes [5, 6], which includes endothelial cell dysfunction causing an increased uptake of lipoproteins, up-regulation of leukocyte adhesion molecules, and leukocyte endothelial transmigration [7, 8]. Generally, the magnitude of WSS varies within a range of 1–7 Pa [5, 9]. Low (< 0.4–0.5 Pa or < 4–5 dyne/cm²) and

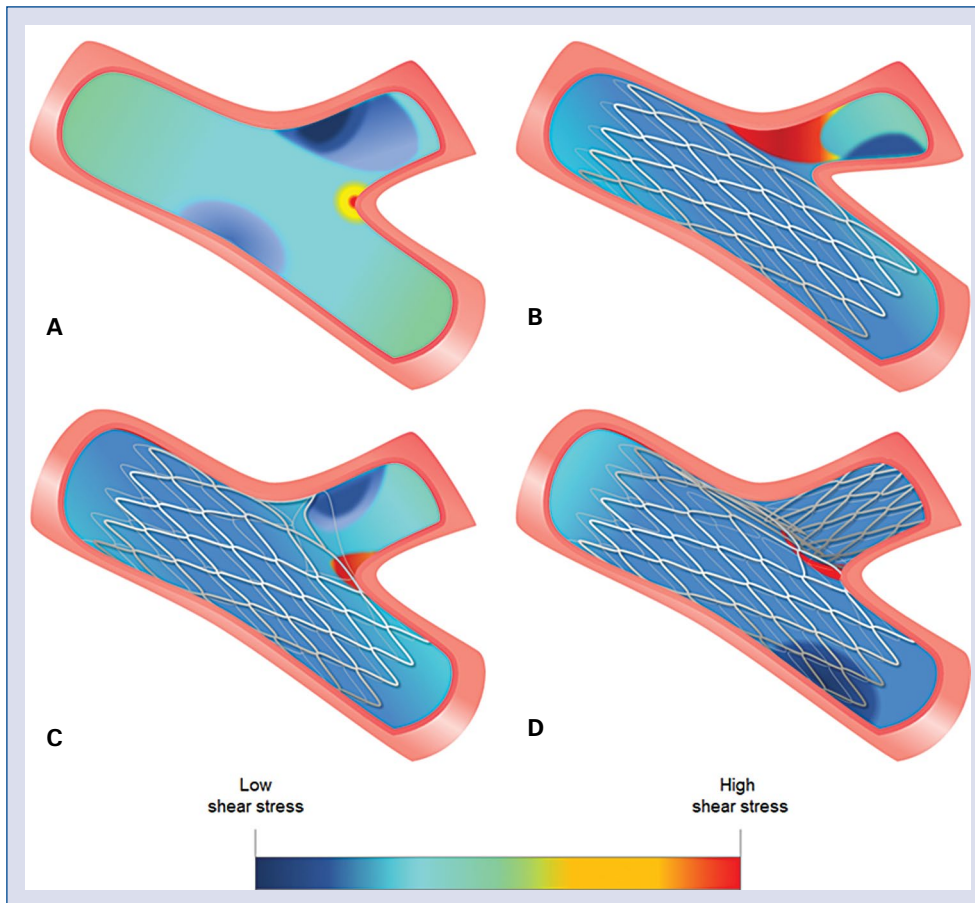


Figure 2. Theoretical local shear stress (SS) distribution in an idealized coronary artery bifurcation before and after stent implantation; **A.** Before stenting (low SS values are present at the level of lateral walls of the main vessel (MV) and the proximal side branch (SB), while high SS values are at the level of the carina and at the internal walls of the distal MV and SB); **B.** After stent implantation in the MV without intervention on the SB; **C.** After MV stenting followed by kissing balloon inflation with short balloons selected in order to avoid proximal MV overstretch; **D.** After the double stenting technique.

oscillatory WSS is considered pro-atherogenic, whereas higher WSS, ranging between 1 and 7 Pa, is considered athero-protective [6, 9]. High WSS (> 7 Pa) has pro-thrombotic potential [5, 9].

A bifurcation divides the blood flow and modifies the blood flow velocity profile. As explained by Finet et al. [10], a bifurcation causes incoming blood flow to deviate from its initial streamline in the mother vessel with a skewed velocity profile, where higher speeds are on the internal parts of the SB in continuity with the carina and low and oscillatory WSS in the arterial walls facing the carina. Such a disturbed laminar flow creates areas with reversed flow (i.e., flow separation, recirculation and reattachment to forward flow) or circumferential swirling, which promotes atherogenesis [11].

In summary, as shown in Figure 2A, low and oscillatory SS areas are typically located at the

lateral walls of the MV and SB, while carina is characterized by high SS. Both low and oscillatory WSS constitute a pro-atherogenic local factor contributing to initiation and progression of atherosclerosis [12]. Furthermore, it has been noted that the location of focal elevated WSS can be often matched with the plaque rupture site [13]. Therefore, the relationship between WSS and atherosclerosis is reciprocal, since plaque formation leads to blood flow perturbation, which results in local SS alteration. WSS inhomogeneity tends to increase with an increase of the bifurcation angle and SB diameter. In particular, a wide angle between MV and SB intensifies flow perturbations, increases the spatial WSS variations in the bifurcation region and low WSS in the lateral walls: the higher the angle and diameter the lower the WSS. The aforementioned may promote atherosclerosis development [11, 14].

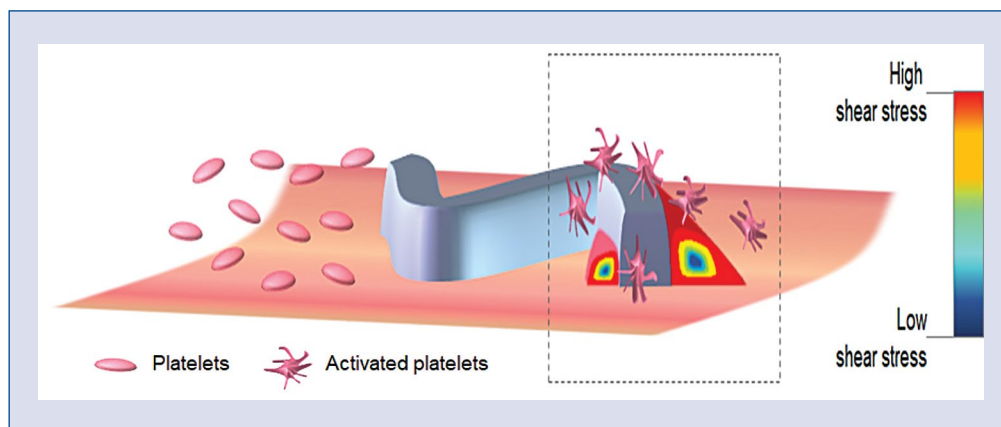


Figure 3. Local shear stress distribution around the stent struts and their possible interactions with circulating platelets. Regions of low shear stress are localized around stent struts and are associated with stagnation flow and boundary layer separation immediately upstream and downstream of the struts.

Table 1. Key hemodynamic parameters assessed in coronary stenting procedures [5, 6, 9, 17–20].

	Relevant values/thresholds identified in biological studies	Main biological effects in stented regions
Time-averaged wall shear stress (TAWSS)	Low TAWSS: < 0.4 Pa High TAWSS: > 20–25 Pa	Low TAWSS associated with an increased risk of neointima hyperplasia and inflammation High TAWSS associated with fibrin deposition and stent struts uncoverage
Oscillatory shear index (OSI)	High OSI: > 0.2	High OSI associated with an increased risk of neointima hyperplasia, inflammation, thrombosis
Relative residence time (RRT)	High RRT: > 4.17 Pa ⁻¹	High RRT associated with neointima hyperplasia and thrombus formation

Local flow modifications after stent implantation

Drug-eluting stent implantation, as with any current stenting procedure, affects the regional arterial geometry, and consequently alters local flow conditions. These flow changes are represented by low WSS, flow recirculation, blood flow separation created by stent struts, and prolonged particulate residence time.

The idealized local flow perturbation at the stent strut/vessel wall level is depicted in Figure 3. These stent-induced disturbances of blood flow contribute to complex spatiotemporal alterations in WSS, which lead to increased thrombogenicity around the stent struts and changes in endothelial phenotype that promote inflammatory cell migration [15]. Simulations of blood flow in the vicinity of stent struts in vessel models determine the effect

of model strut geometries upon the generation of prothrombotic conditions that are mediated by flow perturbations [16]. Furthermore, changes in local WSS distribution are responsible for the vascular smooth muscle cells proliferative and migratory responses that lead to neointimal hyperplasia and restenosis [17].

The major hemodynamic parameters that have been assessed at stented coronary bifurcations through computational fluid dynamics simulations are: time-averaged wall shear stress (TAWSS), oscillatory shear index (OSI) and relative residence time (RRT) (Table 1). TAWSS expresses the frictional force per unit area that is exerted by the blood flowing to the vascular wall due to viscous properties of blood averaged in a cardiac cycle [18]. OSI is a dimensionless parameter that accounts for the degree of deviation of WSS from the antegrade flow direction [18–20], used to identify regions on

the vessel wall subjected to highly oscillating wall shear stress directions during the cardiac cycle. RRT is an index of flow derived from TAWSS and OSI that measures how long the particles stay near the wall of the vessel [18]. High values of RRT indicate that residence time of particles near the wall is prolonged [21] with the possibility of inducing ISR [19]. Furthermore, thrombus formation is enhanced at areas of slow and reversed flow characterized by high OSI and high RRT [18].

The insertion of a stent in bifurcation affects local fluid dynamics. Indeed, stent architecture and stent strut profile have a significant impact on fluid dynamics and drug transport in the arterial wall. In particular, increasing strut thickness and number of stent struts resulted in an increase of area exposed to low WSS [17]. This has recently been confirmed by a biomechanical analysis, whose results corroborate the findings of the large-scale ISAR STEREO clinical trials and highlight the crucial role of strut thickness in coronary stent design [22]. Moreover, streamlined stent structure profiles (e.g. elliptical and tear-drop) exhibit better hemodynamic performance compared to the standard square or circular profiles since the streamlined ones have smaller recirculation zones and a lower percentage of inter-strut area where the WSS level is decreased [8]. In cases of stent malapposition, or incomplete stent apposition, stent struts resulted in separation from the intimal surface of the arterial wall with evidence of blood behind the strut. Malapposed stent struts disrupt the laminar flow and can generate regions of high shear stress, which are known to facilitate the development of stent thrombosis [8].

Flow modifications after stenting in bifurcations

The complex local flow microenvironment generated during PCI with stent implantation at the level of coronary bifurcations may also influence ISR, ST and clinical outcomes [23]. In bifurcation stenting, there is an increased rate of restenosis and a higher risk of late stent thrombosis. In DES most of the thrombi originate at the flow divider sites where uncovered struts are more frequently observed [12], while ISR has been shown to be associated with low WSS [8, 17].

Pathologic studies have shown that eccentric neointimal hyperplasia occurs predominantly at the lateral wall of the stented MV of a coronary bifurcation, with concomitant adhesion and accumulation of leukocytes, whereas the carina is almost completely free of leukocytes [24].

Yazdani et al. [7], using *in vitro* experimental bifurcation models, demonstrated that deployment of stents can alter boundary layer separation of the lateral walls and can produce flow disturbances (vortical structures) at the carina. Regions of boundary layer separation were associated with low WSS, poor mass transfer of blood flow and an increase in residence time of circulating blood elements. Furthermore, the development of vortical structures can prolong and alter areas with low WSS and can influence drug deposition, arterial healing post-stenting, and local fibrin and platelet deposition.

In cases of DES, recirculation zones with reduced flow and low WSS prolongs residence time and increases local concentration of the eluted compound. In such regions with decelerated flow, the locally augmented anti-proliferative drug effect might thereby antagonize the pro-restenotic effect of low WSS per se [8]. Consequently, this inflammatory response at the lateral walls suggests that there is a specific link among local low WSS, inflammation and focal ISR.

Moreover, stent complications such as malapposition, under-expansion, edge dissections and intra-stent tissue prolapse are often detected in patients successfully treated by bifurcation stenting [25]. Such “imperfections” may theoretically contribute to less optimal stenting outcomes in bifurcation interventions. For example, implantation of two overlapping stents substantially reduces WSS downstream of the junction as compared with a single longer stent, likely indicating a region prone to re-narrowing at the overlap zone [8].

Impact of stenting techniques on bifurcation fluid dynamics

Percutaneous coronary intervention procedures for coronary bifurcations can utilize different technique for stenting [26]. The simplest stent technique is the provisional SB stenting technique, which uses one stent in the MV, eventually followed by further interventions (like ballooning and/or stenting) in the SB. Conversely, double stenting techniques comprise many different techniques involving the use of stents in both the MV and the SB [26].

Despite numerous clinical and computational studies, the effect of each stent implantation method on the coronary artery hemodynamic is not well understood. To date, studies on bifurcation stenting fluid dynamics have been conducted by *in vitro* bench testing and computational simulations.

Computational fluid dynamics (CFD) is a powerful emerging tool since it offers the possibility to investigate local hemodynamics of non-stented and stented coronary artery bifurcations at a level of detail not easily accessed with experimental techniques [27, 28]. Computer simulations can assess the local hemodynamic microenvironment in bifurcations, pre- and post-stenting, providing an insight into the role of local hemodynamic stresses on neointimal hyperplasia and stent thrombosis [4].

Fluid dynamics in provisional technique

In coronary bifurcations, MV stenting restores main lumen and creates side-cell strut jailing at the level of SB ostium. This implies a peculiar pattern of flow in the coronary bifurcation characterized by a pronounced velocity jet in the SB with vortices extending from jailed struts into the SB and causing eccentric areas of low velocity on the main lateral wall away from the carina and in the SB distal to the carina (Fig. 2B).

Side branch ballooning is able to reduce (if present), ostial SB residual stenosis and remove stent struts from the SB ostium. According to computer simulations, this creates a more concentric region of low velocity in the MV distal to the carina and an area of low velocity in the SB lateral wall [29]. However, the total area of the luminal surface exposed to low TAWSS is essentially the same before and after SB balloon angioplasty [29]. In other words, although post-stenting SB angioplasty provides an excellent result in terms of SB patency (from a fluid dynamics perspective), there are only modest differences especially in the MV, indicating that a potential for MV ISR or ST may be unchanged.

Interestingly, the course of time may play an important role in flow alterations after bifurcation stenting. Zhang et al. [30] observed that both the reduction of WSS in the lateral wall of MV and an increase of WSS in SB would predict no restenosis 8 months after stenting of true bifurcation lesions by the provisional SB technique with SB ballooning. Over time, flow tends to return to its original pattern before PCI with high WSS in the internal wall and low WSS in the lateral wall. Yet, proliferation inhibition related to DES implantation may be sufficient to prevent the development of significant restenosis.

Another important issue is related to the technique for SB ballooning. Typically, kissing balloon inflation is commonly selected since it prevents major MV stent distortion [31]. Yet, it is now known that kissing balloon inflation has different consequences according to the stent's side-cells that are crossed with the wire and the balloon [32, 33].

In summary, the pattern of stent strut removal (and consequently the turbulence generated by the presence of residual jailing struts) may differ during kissing balloon inflation practice making its influence on SB flow somewhat unpredictable. Another important issue related with kissing ballooning is represented by its potential to induce MV overstretch. A CFD study documented that after kissing balloon inflation, a wider region characterized by low WSS in the proximal part of the MV was induced [34]. As a consequence of such proximal MV overstretch, the percentage of lumen area of the stented region exposed to WSS lower than 0.5 Pa was 79.0% after kissing as compared to 62.3% before the kissing balloon [34].

In conclusion, kissing balloon inflation (when performed after distal SB rewiring) may restore a better SB flow (with reduced accelerations and recirculation related with SB ostial stenosis and jailing stent struts) but has marginal or even adverse impact on MV shear stress (Fig. 2C).

Fluid dynamics in two-stent techniques

Double stenting specific techniques have been developed with the aim of improving the angiographic result in both the MV and the SB. However, the double stenting technique failed to show improved outcomes in clinical trials and hence these techniques are not recommended for unselected bifurcated coronary lesions [35]. The search for technical refinements in double stenting is ongoing and technical innovations may offer promising results [36]. All double stenting techniques have the potential for stent malapposition areas, which may influence local fluid dynamics. In a bench test study comparing different double stenting techniques, the crush technique resulted in a higher risk of malapposition than either the culotte or T-/TAP technique [37].

Due to different areas of double layers of struts and malapposed stent struts, each double stenting technique has a distinct impact on the flow patterns. Nevertheless, all double-stenting techniques failed to improve the fluid dynamics result over provisional. According to Raben et al. [38], double-stented cases (culotte, crush and T-stenting technique with high protrusion) showed a detrimental influence of multiple metallic layers on WSS. In particular, low flow regions protruding toward the centerline of the MV and following the distal surface of the SB stent were observed. In the double-stented models, the simultaneous presence of two devices led to the creation of a metallic carina between the SB and the distal part of the

MV, in addition to the presence of a larger number of stent struts at the flow divider. The disturbance created by this geometry led to low velocity and WSS as well as high shear stress in and around the region of the flow divider and in the proximal MV (Fig. 2D). Unapposed struts in the neocarina cause severe flow disturbances with a high shear rate that may increase the risk of platelet adhesion and stent thrombosis [37].

In a study by Brindise et al. [39], three different stenting techniques were compared in four compliant coronary artery models with a 60° bifurcation: provisional, crush and culotte technique. Overall, the culotte technique resulted in minimal stent induced flow disturbances as compared with the crush technique. Moreover, the culotte technique mitigated detrimental effects induced by a high bifurcation angle.

These observations, however, have not been confirmed by any further studies. In the study by Katritsis et al. [18], the crush technique with the use of a thin-strut stent resulted in improved hemodynamics compared with culotte or T-stenting, which had the most favourable fluid dynamics. Furthermore, the “nano-crush” and modified T techniques seem to restore the most physiologic fluid dynamic patterns (with the lowest values of WSS) with the addition of a final proximal optimization technique appears to be a favourable step [40].

Finally, it has been noted that SB stent length, in a setting of double stenting techniques, may have impact on local fluid dynamics during double stenting techniques. A longer SB stent adversely affects the hemodynamics of the SB by inducing lower WSS and higher OSI in the SB [41].

In summary, the double stenting technique is expected to induce blood flow perturbations which are not completely predictable and probably depend from the type and length of selected stents, specific sequence for their implantation and final result achieved. These issues, which are well recognized in experimental setting, are expected to be even more pronounced in clinical practice. This is because stent/vessel interactions, during each technical step of the complex sequences needed for double stenting, are not entirely predictable in clinical settings.

Conclusions and future perspectives

Coronary bifurcations represent common target lesions in contemporary PCI practice. DES improved clinical results of PCI on bifurcated lesions but they still represent a technical challenge gravely by higher clinical risks. As a consequence,

interventional management of bifurcation lesions is an evolving field [4]. Fluid-dynamic perturbations are known to be increased at the level of stents implanted at bifurcated lesions and have, theoretically, potential impact on stent healing.

Currently, the possibility to create highly accurate three-dimensional geometrical models of coronary bifurcations that include a precise fidelity of stent geometry has become a reality [28]. The application of CFD simulation algorithms to such reconstructions allows the collecting of detailed flow-related hemodynamic force evaluation and local microenvironment assessment following bifurcation stenting. Post-PCI fluid dynamics is dependent on a series of factors including stent selection, stent implantation technique, and bifurcation geometry. CFD from patient-specific models may represent a powerful tool in calculating local fluid dynamics quantity, such as WSS, to guide and optimize PCI strategies in order to predict adverse events and improve clinical outcomes. Therefore, effort should be made to optimize stent deployment and stent/scaffold design to ensure an optimal hemodynamic profile and reduce the risk of complications after PCI. Integration of this data and analysis may help improve the identification of both “tailored” PCI strategies and device improvements. In particular, CFD simulations can theoretically be used as a tool to guide both bifurcation stenting strategy and selection of the stenting technique with optimal post-PCI flow conditions in this challenging setting. In conclusion, patient-level CFD modeling has the potential to recover a critical role for the future improvement of bifurcation PCI and the integration of this tool with others to assess hemodynamic parameters which could guide future coronary bifurcation treatment.

Conflict of interest: Dr. Carlo Trani disclose to have received speaker fees from Medtronic, Abbott, Abiomed; Dr. Francesco Burzotta disclose to have received speaker fees from Medtronic, Abbott, Abiomed; Other Authors — None declared

References

1. Lassen JF, Burzotta F, Banning AP, et al. Percutaneous coronary intervention for the left main stem and other bifurcation lesions: 12th consensus document from the European Bifurcation Club. *EuroIntervention*. 2018; 13(13): 1540–1553, doi: [10.4244/EIJ-D-17-00622](https://doi.org/10.4244/EIJ-D-17-00622), indexed in Pubmed: [29061550](https://pubmed.ncbi.nlm.nih.gov/29061550/).
2. Sawaya FJ, Lefèvre T, Chevalier B, et al. Contemporary approach to coronary bifurcation lesion treatment. *JACC Cardiovasc Interv*. 2016; 9(18): 1861–1878, doi: [10.1016/j.jcin.2016.06.056](https://doi.org/10.1016/j.jcin.2016.06.056), indexed in Pubmed: [27659563](https://pubmed.ncbi.nlm.nih.gov/27659563/).

3. Park TK, Park YH, Song YB, et al. Long-Term clinical outcomes of true and non-true bifurcation lesions according to Medina classification- results from the COBIS (COronary Bifurcation Stent) II registry. *Circ J*. 2015; 79(9): 1954–1962, doi: [10.1253/circj.CJ-15-0264](https://doi.org/10.1253/circj.CJ-15-0264), indexed in Pubmed: [26134457](https://pubmed.ncbi.nlm.nih.gov/26134457/).
4. Antoniadis AP, Mortier P, Kassab G, et al. Biomechanical modeling to improve coronary artery bifurcation stenting: expert review document on techniques and clinical implementation. *JACC Cardiovasc Interv*. 2015; 8(10): 1281–1296, doi: [10.1016/j.jcin.2015.06.015](https://doi.org/10.1016/j.jcin.2015.06.015), indexed in Pubmed: [26315731](https://pubmed.ncbi.nlm.nih.gov/26315731/).
5. Chatzizisis YS, Coskun AU, Jonas M, et al. Role of endothelial shear stress in the natural history of coronary atherosclerosis and vascular remodeling: molecular, cellular, and vascular behavior. *J Am Coll Cardiol*. 2007; 49(25): 2379–2393, doi: [10.1016/j.jacc.2007.02.059](https://doi.org/10.1016/j.jacc.2007.02.059), indexed in Pubmed: [17599600](https://pubmed.ncbi.nlm.nih.gov/17599600/).
6. Morbiducci U, Kok AM, Kwak BR, et al. Atherosclerosis at arterial bifurcations: evidence for the role of haemodynamics and geometry. *Thromb Haemost*. 2016; 115(3): 484–492, doi: [10.1160/TH15-07-0597](https://doi.org/10.1160/TH15-07-0597), indexed in Pubmed: [26740210](https://pubmed.ncbi.nlm.nih.gov/26740210/).
7. Yazdani SK, Nakano M, Otsuka F, et al. Atheroma and coronary bifurcations: before and after stenting. *EuroIntervention*. 2010; 6 Suppl J: J24–J30, doi: [10.4244/EIJV6SUPJA5](https://doi.org/10.4244/EIJV6SUPJA5), indexed in Pubmed: [21930487](https://pubmed.ncbi.nlm.nih.gov/21930487/).
8. Koskinas KC, Chatzizisis YS, Antoniadis AP, et al. Role of endothelial shear stress in stent restenosis and thrombosis: pathophysiologic mechanisms and implications for clinical translation. *J Am Coll Cardiol*. 2012; 59(15): 1337–1349, doi: [10.1016/j.jacc.2011.10.903](https://doi.org/10.1016/j.jacc.2011.10.903), indexed in Pubmed: [22480478](https://pubmed.ncbi.nlm.nih.gov/22480478/).
9. Malek AM, Alper SL, Izumo S. Hemodynamic shear stress and its role in atherosclerosis. *JAMA*. 1999; 282(21): 2035–2042, doi: [10.1001/jama.282.21.2035](https://doi.org/10.1001/jama.282.21.2035), indexed in Pubmed: [10591386](https://pubmed.ncbi.nlm.nih.gov/10591386/).
10. Finet G, Huo Y, Rioufol G, et al. Structure-function relation in the coronary artery tree: from fluid dynamics to arterial bifurcations. *EuroIntervention*. 2010; 6 (Suppl J): J10–J15, doi: [10.4244/EIJV6SUPJA3](https://doi.org/10.4244/EIJV6SUPJA3), indexed in Pubmed: [21930472](https://pubmed.ncbi.nlm.nih.gov/21930472/).
11. Giannoglou GD, Antoniadis AP, Koskinas KC, et al. Flow and atherosclerosis in coronary bifurcations. *EuroIntervention*. 2010; 6 (Suppl J): J16–J23, doi: [10.4244/EIJV6SUPJA4](https://doi.org/10.4244/EIJV6SUPJA4), indexed in Pubmed: [21930484](https://pubmed.ncbi.nlm.nih.gov/21930484/).
12. Antoniadis AP, Giannopoulos AA, Wentzel JJ, et al. Impact of local flow haemodynamics on atherosclerosis in coronary artery bifurcations. *EuroIntervention*. 2015; 11 (Suppl V): V18–V22, doi: [10.4244/EIJV11SVA4](https://doi.org/10.4244/EIJV11SVA4), indexed in Pubmed: [25983161](https://pubmed.ncbi.nlm.nih.gov/25983161/).
13. Fukumoto Y, Hiro T, Fujii T, et al. Localized elevation of shear stress is related to coronary plaque rupture: a 3-dimensional intravascular ultrasound study with in-vivo color mapping of shear stress distribution. *J Am Coll Cardiol*. 2008; 51(6): 645–650, doi: [10.1016/j.jacc.2007.10.030](https://doi.org/10.1016/j.jacc.2007.10.030), indexed in Pubmed: [18261684](https://pubmed.ncbi.nlm.nih.gov/18261684/).
14. Huo Y, Finet G, Lefevre T, et al. Which diameter and angle rule provides optimal flow patterns in a coronary bifurcation? *J Biomech*. 2012; 45(7): 1273–1279, doi: [10.1016/j.jbiomech.2012.01.033](https://doi.org/10.1016/j.jbiomech.2012.01.033), indexed in Pubmed: [22365499](https://pubmed.ncbi.nlm.nih.gov/22365499/).
15. Otsuka F, Finn AV, Yazdani SK, et al. The importance of the endothelium in atherothrombosis and coronary stenting. *Nat Rev Cardiol*. 2012; 9(8): 439–453, doi: [10.1038/nrcardio.2012.64](https://doi.org/10.1038/nrcardio.2012.64), indexed in Pubmed: [22614618](https://pubmed.ncbi.nlm.nih.gov/22614618/).
16. Jiménez JM, Prasad V, Yu MD, et al. Macro- and microscale variables regulate stent haemodynamics, fibrin deposition and thrombomodulin expression. *J R Soc Interface*. 2014; 11(94): 20131079, doi: [10.1098/rsif.2013.1079](https://doi.org/10.1098/rsif.2013.1079), indexed in Pubmed: [24554575](https://pubmed.ncbi.nlm.nih.gov/24554575/).
17. Wentzel JJ, Gijsen FJH, Schuurbiers JCH, et al. The influence of shear stress on in-stent restenosis and thrombosis. *EuroIntervention*. 2008; 4 (Suppl C): C27–C32, indexed in Pubmed: [19202688](https://pubmed.ncbi.nlm.nih.gov/19202688/).
18. Katritsis DG, Theodorakakos A, Pantos I, et al. Flow patterns at stented coronary bifurcations: computational fluid dynamics analysis. *Circ Cardiovasc Interv*. 2012; 5(4): 530–539, doi: [10.1161/CIRCINTERVENTIONS.112.968347](https://doi.org/10.1161/CIRCINTERVENTIONS.112.968347), indexed in Pubmed: [22763345](https://pubmed.ncbi.nlm.nih.gov/22763345/).
19. Chiastra C, Morlacchi S, Gallo D, et al. Computational fluid dynamic simulations of image-based stented coronary bifurcation models. *J R Soc Interface*. 2013; 10(84): 20130193, doi: [10.1098/rsif.2013.0193](https://doi.org/10.1098/rsif.2013.0193), indexed in Pubmed: [23676893](https://pubmed.ncbi.nlm.nih.gov/23676893/).
20. Chiastra C, Gallo D, Tasso P, et al. Healthy and diseased coronary bifurcation geometries influence near-wall and intravascular flow: A computational exploration of the hemodynamic risk. *J Biomech*. 2017; 58: 79–88, doi: [10.1016/j.jbiomech.2017.04.016](https://doi.org/10.1016/j.jbiomech.2017.04.016), indexed in Pubmed: [28457603](https://pubmed.ncbi.nlm.nih.gov/28457603/).
21. Pinto SIS, Campos JB. Numerical study of wall shear stress-based descriptors in the human left coronary artery. *Comput Methods Biomech Biomed Engin*. 2016; 19(13): 1443–1455, doi: [10.1080/10255842.2016.1149575](https://doi.org/10.1080/10255842.2016.1149575), indexed in Pubmed: [26883291](https://pubmed.ncbi.nlm.nih.gov/26883291/).
22. Martin D, Boyle F. Sequential structural and fluid dynamics analysis of balloon-expandable coronary stents: a multivariable statistical analysis. *Cardiovasc Eng Technol*. 2015; 6(3): 314–328, doi: [10.1007/s13239-015-0219-9](https://doi.org/10.1007/s13239-015-0219-9), indexed in Pubmed: [26577363](https://pubmed.ncbi.nlm.nih.gov/26577363/).
23. Van der Heiden K, Gijsen FJH, Narracott A, et al. The effects of stenting on shear stress: relevance to endothelial injury and repair. *Cardiovasc Res*. 2013; 99(2): 269–275, doi: [10.1093/cvr/cvt090](https://doi.org/10.1093/cvr/cvt090), indexed in Pubmed: [23592806](https://pubmed.ncbi.nlm.nih.gov/23592806/).
24. Richter Y, Groothuis A, Seifert P, et al. Dynamic flow alterations dictate leukocyte adhesion and response to endovascular interventions. *J Clin Invest*. 2004; 113(11): 1607–1614, doi: [10.1172/JCI21007](https://doi.org/10.1172/JCI21007), indexed in Pubmed: [15173887](https://pubmed.ncbi.nlm.nih.gov/15173887/).
25. Burzotta F, Talarico GP, Trani C, et al. Frequency-domain optical coherence tomography findings in patients with bifurcated lesions undergoing provisional stenting. *Eur Heart J Cardiovasc Imaging*. 2014; 15(5): 547–555, doi: [10.1093/ehjci/jet231](https://doi.org/10.1093/ehjci/jet231), indexed in Pubmed: [24255135](https://pubmed.ncbi.nlm.nih.gov/24255135/).
26. Louvard Y, Thomas M, Dzavik V, et al. Classification of coronary artery bifurcation lesions and treatments: time for a consensus! *Catheter Cardiovasc Interv*. 2008; 71(2): 175–183, doi: [10.1002/ccd.21314](https://doi.org/10.1002/ccd.21314), indexed in Pubmed: [17985377](https://pubmed.ncbi.nlm.nih.gov/17985377/).
27. Migliavacca F, Chiastra C, Chatzizisis YS, et al. Virtual bench testing to study coronary bifurcation stenting. *EuroIntervention*. 2015; 11 (Suppl V): V31–V34, doi: [10.4244/EIJV11SVA7](https://doi.org/10.4244/EIJV11SVA7), indexed in Pubmed: [25983167](https://pubmed.ncbi.nlm.nih.gov/25983167/).
28. Chiastra C, Migliori S, Burzotta F, et al. Patient-Specific modeling of stented coronary arteries reconstructed from optical coherence tomography: towards a widespread clinical use of fluid dynamics analyses. *J Cardiovasc Transl Res*. 2018; 11(2): 156–172, doi: [10.1007/s12265-017-9777-6](https://doi.org/10.1007/s12265-017-9777-6), indexed in Pubmed: [29282628](https://pubmed.ncbi.nlm.nih.gov/29282628/).
29. Williams AR, Koo BK, Gundert TJ, et al. Local hemodynamic changes caused by main branch stent implantation and subsequent virtual side branch balloon angioplasty in a representative coronary bifurcation. *J Appl Physiol* (1985). 2010; 109(2): 532–540, doi: [10.1152/jappphysiol.00086.2010](https://doi.org/10.1152/jappphysiol.00086.2010), indexed in Pubmed: [20507966](https://pubmed.ncbi.nlm.nih.gov/20507966/).
30. Zhang JJ, Zhang JJ, Chen SL, et al. Contradictory shear stress distribution prevents restenosis after provisional stenting for

- bifurcation lesions. *J Interv Cardiol.* 2010; 23(4): 319–329, doi: [10.1111/j.1540-8183.2010.00572.x](https://doi.org/10.1111/j.1540-8183.2010.00572.x), indexed in Pubmed: [20642478](https://pubmed.ncbi.nlm.nih.gov/20642478/).
31. Sgueglia GA, Chevalier B. Kissing balloon inflation in percutaneous coronary interventions. *JACC Cardiovasc Interv.* 2012; 5(8): 803–811, doi: [10.1016/j.jcin.2012.06.005](https://doi.org/10.1016/j.jcin.2012.06.005), indexed in Pubmed: [22917451](https://pubmed.ncbi.nlm.nih.gov/22917451/).
 32. Burzotta F, Trani C. In bifurcation PCI, as in everyday life, the consequences of kissing may not always be the same. *Euro-Intervention.* 2016; 11(11): e1209–e1213, doi: [10.4244/EI-JV11I11A240](https://doi.org/10.4244/EI-JV11I11A240), indexed in Pubmed: [26865437](https://pubmed.ncbi.nlm.nih.gov/26865437/).
 33. Chiastra C, Morlacchi S, Pereira S, et al. Computational fluid dynamics of stented coronary bifurcations studied with a hybrid discretization method. *Eur J Mech - B/Fluids.* 2012; 35: 76–84, doi: [10.1016/j.euromechflu.2012.01.011](https://doi.org/10.1016/j.euromechflu.2012.01.011).
 34. Morlacchi S, Chiastra C, Gastaldi D, et al. Sequential structural and fluid dynamic numerical simulations of a stented bifurcated coronary artery. *J Biomech Eng.* 2011; 133(12): 121010, doi: [10.1115/1.4005476](https://doi.org/10.1115/1.4005476), indexed in Pubmed: [22206427](https://pubmed.ncbi.nlm.nih.gov/22206427/).
 35. Katritsis DG, Siontis GCM, Ioannidis JPA. Double versus single stenting for coronary bifurcation lesions: a meta-analysis. *Circ Cardiovasc Interv.* 2009; 2(5): 409–415, doi: [10.1161/CIRCINTERVENTIONS.109.868091](https://doi.org/10.1161/CIRCINTERVENTIONS.109.868091), indexed in Pubmed: [20031750](https://pubmed.ncbi.nlm.nih.gov/20031750/).
 36. Chen SL, Zhang JJ, Han Y, et al. Double kissing crush versus provisional stenting for left main distal bifurcation lesions: DKCRUSH-V randomized trial. *J Am Coll Cardiol.* 2017; 70(21): 2605–2617, doi: [10.1016/j.jacc.2017.09.1066](https://doi.org/10.1016/j.jacc.2017.09.1066), indexed in Pubmed: [29096915](https://pubmed.ncbi.nlm.nih.gov/29096915/).
 37. Foin N, Alegria-Barrero E, Torii R, et al. Crush, culotte, T and protrusion: which 2-stent technique for treatment of true bifurcation lesions? - insights from in vitro experiments and micro-computed tomography. *Circ J.* 2013; 77(1): 73–80, doi: [10.1253/circj.cj-12-0272](https://doi.org/10.1253/circj.cj-12-0272), indexed in Pubmed: [23006784](https://pubmed.ncbi.nlm.nih.gov/23006784/).
 38. Raben JS, Morlacchi S, Burzotta F, et al. Local blood flow patterns in stented coronary bifurcations: an experimental and numerical study. *J Appl Biomater Funct Mater.* 2015; 13(2): e116–e126, doi: [10.5301/jabfm.5000217](https://doi.org/10.5301/jabfm.5000217), indexed in Pubmed: [25589159](https://pubmed.ncbi.nlm.nih.gov/25589159/).
 39. Brindise MC, Chiastra C, Burzotta F, et al. Hemodynamics of Stent Implantation Procedures in Coronary Bifurcations: An In Vitro Study. *Ann Biomed Eng.* 2017; 45(3): 542–553, doi: [10.1007/s10439-016-1699-y](https://doi.org/10.1007/s10439-016-1699-y), indexed in Pubmed: [27460012](https://pubmed.ncbi.nlm.nih.gov/27460012/).
 40. Rigatelli G, Zuin M, Dell'Avvocata F, et al. Evaluation of coronary flow conditions in complex coronary artery bifurcations stenting using computational fluid dynamics: Impact of final proximal optimization technique on different double-stent techniques. *Cardiovasc Revasc Med.* 2017; 18(4): 233–240, doi: [10.1016/j.carrev.2017.01.002](https://doi.org/10.1016/j.carrev.2017.01.002), indexed in Pubmed: [28108202](https://pubmed.ncbi.nlm.nih.gov/28108202/).
 41. Chen HY, Koo BK, Kassab GS. Impact of bifurcation dual stenting on endothelial shear stress. *J Appl Physiol (1985).* 2015; 119(6): 627–632, doi: [10.1152/jappphysiol.00082.2015](https://doi.org/10.1152/jappphysiol.00082.2015), indexed in Pubmed: [26183473](https://pubmed.ncbi.nlm.nih.gov/26183473/).